# Bridged or cohesive crack in bending of fibre-reinforced beams

**A. Carpinteri, G. Ferro, G. Ventura**

Politecnico di Torino, Department of Structural Engineering and Geotechnics, 10129 Torino, Italy.

*ABSTRACT: A dimensionless formulation is proposed of the bridged or the cohesive crack model for reproducing the constitutive flexural response of a reinforced concrete element with a nonlinear matrix. The nonlinearity of the matrix is modelled by considering a distribution of closing forces onto the crack faces which increases the fracture toughness of the cross-section with a shielding action. The peculiarity of the models consists in the imposition of both the equilibrium and the compatibility conditions to the cracked element. The constitutive flexural response depends on three dimensionless parameters: $\tilde{w}_c$, which controls the extension of the process zone, $N_P^{(1)}$ and $N_P^{(2)}$, which are related to the reinforcement phases.*

## INTRODUCTION

High-strength concretes result very promising for the realization of large structures, even if they show a very brittle behaviour. The role of fibers, or secondary reinforcement, is to control the crack growth by the bridging actions on the micro- and macro-cracks of the cementitious matrix. On the other hand, the primary reinforcements (longitudinal bars) play a fundamental role when a macrocrack is formed and propagates along the cross-section.

Interesting developments for these materials are related to the progresses in Fracture Mechanics. In fact, the application of Fracture Mechanics concepts to plain and reinforced concrete structures represents the only way to interpret the collapse behaviour, which shows different rupture modes by varying the size. Two different models have been proposed to describe partial damage near a single crack: the *cohesive* and the *bridged* crack model. In the former, the stress-intensity factor (SIF) $K_I$ at the crack tip is set equal to zero due to the contribution of the applied load and to the softening tractions acting ahead of the notch. The first application to brittle materials is due to Barenblatt [1], while important contributions are due to Willis [2] and Rice [3]. In the latter, the mean tip process is modeled via the SIF and a crack propagation condition is reached when the SIF equals the toughness of the brittle matrix.

The model presented in this paper simulates the action of two different levels of reinforcements onto the cracked cross-section of a structural member in bending. It constitutes an extension of previous models proposed by the first author for reinforced concrete with only one reinforcement [4, 5], for a discrete distribution of reinforcements [6, 7] and for a continuous distribution of fibers [8, 9, 10]. The present model, valid for cementitious materials, can also be applied to a wider class of composite materials [11].

## THEORETICAL MODELS

The theoretical model explains and reproduces the constitutive flexural response of a fiber-reinforced concrete element with longitudinal steel bars. Two different options for the model can be used, the $bridging$ and the $cohesive$. The scheme of a cracked element is shown in fig.1, where $h$ and $b$ are the height and the thickness of the cross-section. The normalized crack depth $\xi = a/h$ and the normalized coordinate $\zeta = x/h$ are defined, $x$ being the coordinate related to the bottom of the cross-section. In the bridging option, the distribution of the discrete actions $P_i$ and of the continuous closing tractions $\sigma(w)$, directly applied onto the crack faces, represent the physical bridging mechanisms respectively of the longitudinal bars (primary reinforcement) and of the fibers (secondary reinforcement), acting at two different scales. $c_i$ is the coordinate of the $i^{th}$ reinforcement from the bottom of the beam, and $\zeta_i = c_i/h$ its normalized value. Function $\sigma(w)$ is a constitutive law and defines the relation between the bridging traction, representative of the action exerted by the fibers onto the crack, and $w(x)$, the crack opening displacement at the generic coordinate $x$. The bridging forces of the secondary reinforcement act on the portion of the crack where the opening displacement is less than its critical value $w_c$. When $w > w_c$ the closing tractions vanish. In the cohesive option, on the other hand, the brittle matrix and the fibers are represented as a single-phase material with homogenized properties. In this case, the closing tractions $\sigma(w)$ describe the combined restraining action of matrix and fibers on the crack opening and are given by the cohesive law of the composite material. The assumed rigid-plastic bridging relation for the crack opening displacement $w_i$ at the level

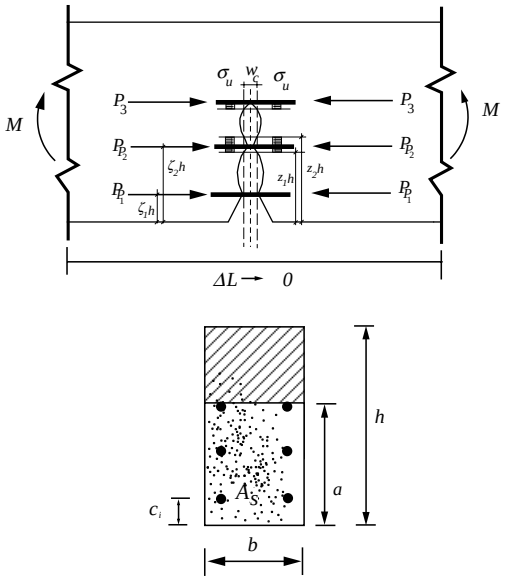


**Figure** 1. Scheme of a cracked reinforced concrete element containing fibers.

of the $i^{th}$ reinforcement is suitable to describe the yielding mechanism of the reinforcement as well as the bar-matrix relative slippage. The maximum bridging traction is defined for the primary reinforcements by the ultimate force $P_{P_i} = A_i\sigma_y$ and for the fibers by the ultimate stress $\sigma_0 = \gamma\sigma_u$, $A_i$ being the single reinforcement cross-section area, $\gamma$ the fiber volume ratio, $\sigma_y$ or $\sigma_u$ the minimum between the reinforcement yield strength and the sliding limit for the two reinforcement phases. The stress-intensity factors, $K_{IM}$ due to the bending moment $M_F$, $K_{I\sigma}$ due to the fibers and $K_{Ij}$ due to the $i^{th}$-longitudinal reinforcement, can be expressed in accordance with the two-dimensional single-edge notched-strip solution:

$$\begin{aligned} &K_{IM} = \frac{M}{bh^{1.5}} Y_M(\xi); \quad K_{I\sigma} = \frac{1}{h^{0.5}b}\int_0^{\xi} \sigma(w(\zeta)) Y_P(\xi,\zeta) bh \, \mathrm{d}\zeta; \\ &K_{Ii} = \frac{P_i}{bh^{0.5}} Y_P(\xi,\zeta_i) \quad (i = 1,\, 2,\, ....., m), \end{aligned} \tag{1}$$

where $Y_M(\xi)$ and $Y_P(\xi,\zeta_i)$ are function of the relative crack depth $\xi$ [13, 14]. The crack propagates when $K_I$ is equal to the matrix toughness, $K_{IC}$, for the $bridging$ option, and when $K_I$ vanishes for the $cohesive$ option:

$$K_I = K_{IM} - \sum_{j=1}^{m} K_{Ij} - K_{I\sigma} = \begin{cases} K_{IC}, & \text{bridging option;} \\ 0, & \text{cohesive option.} \end{cases} \tag{2}$$

The dimensionless crack propagation moment can be obtained from eqs (1):

$$\frac{M_F}{K_{IC}bh^{1.5}} = \frac{1}{Y_M(\xi)} \left\{ \frac{N_P^{(1)}}{\rho} \sum_{i=1}^{m} \rho_i \frac{P_i}{P_{P_i}} Y_P(\xi,\zeta_i) + N_P^{(2)} \int_0^{\xi} \frac{\sigma(w(\zeta))}{\sigma_0} Y_P(\xi,\zeta) bh \, \mathrm{d}\zeta + K \right\}, \tag{3}$$

with

$$N_P^{(2)} = \frac{\gamma\sigma_u h^{0.5}}{K_{IC}} = \frac{\sigma_0 h^{0.5}}{K_{IC}}, \qquad \text{for } K = 1 \;\; (\text{bridging option}), \tag{4}$$

$$N_P^{(2)} = \frac{1}{s} = \frac{\sigma_0 h^{0.5}}{K_{IC}}, \quad \text{for } K = 0 \;\; (\text{cohesive option}), \tag{5}$$

where $s$ is the brittleness number originally defined by Carpinteri [4], and:

$$N_P^{(1)} = \frac{\rho\sigma_y h^{0.5}}{K_{IC}}. \tag{6}$$

The parameters in the two cases assume a different physical meaning. In the bridging option, $K_{IC}$ represents the matrix fracture toughness while in the cohesive it represents the homogenized toughness of the composite; $\sigma_u$ represents the ultimate strength of the secondary reinforcement in the former case while $\sigma_0$ represents the homogenized ultimate strength in the latter. The complete theoretical formulation can be found in [11, 12].

The analytical formulation can be also developed in a dimensionless form to define the parameters that synthetically control the behaviour of the cross-section in bending. A fundamental set of dimensionally independent variables has been chosen, i.e. $K_{IC}$ [F][L]$^{-1.5}$ and $h$ [L]. The dimensionless groups, $K_{IC}/(\sigma_u h^{0.5})$ and $M_F/(K_{IC} h^{1.5} b)$, have been obtained by multiplying the different variables involved in the physical problem by a suitable combination of the fundamental set. When a generic bridging or cohesive law with a critical crack opening displacement $w_c$ is considered, the problem is statically indeterminate and the compatibility must be satisfied. To define the parameters controlling the behaviour for the above assumption, reference should be made to the propagation condition for the traction-free crack, which controls the extension of the bridging or cohesive zone. The traction-free crack propagates when the crack opening diplacement reaches the critical value $w_c$. Such a condition is verified at each iteration of the procedure [11]. It refers the fact that, for an assigned generic bridging or cohesive law, if geometrical similarity is assumed, another dimensionless parameter, i.e.:

$$\tilde{w}_c = \frac{E w_c}{K_{IC} h^{0.5}}, \tag{7}$$

controls the composite flexural response. The functional constitutive relationship can be given the general form [15]:

$$f\left(\frac{M}{K_{IC} h^{1.5}}, \phi, N_P^{(1)}, N_P^{(2)}, \tilde{w}_c\right) = 0. \tag{8}$$

This relation has a general validity for both the model options. Nevertheless, for the cohesive option, the brittleness number $N_P^{(2)} = 1/s$ and the parameter $\tilde{w}_c$ are not independent variables. This is due to the relationship between the homogenized fracture toughness $K_{IC}$ of matrix and secondary phase reinforcement, and the fracture energy $\mathcal{G}_F$. The composite fracture toughness is, in other words, linked, through Irwin's relationship, to the composite fracture energy, which is defined by the area beneath the cohesive curve $\sigma(w)$. Relations between $\tilde{w}_c$ and $N_P^{(2)} = 1/s$ are reported in [11] for different cohesive laws. As a consequence, the dimensionless functional relationship (8) for the cohesive model becomes:

$$f\left(\tilde{M}, \phi, N_P^{(1)}, N_P^{(2)}\right) = 0, \tag{9}$$

where $N_P^{(1)}$ and $N_P^{(2)}$ are the governing parameters.

In conclusion, if the theoretical problem is analyzed via the bridging option of the proposed model, and the material is modeled as multiphase, three parameters, $N_P^{(1)}$, $N_P^{(2)}$ and $\tilde{w}_c$ control the mechanical response of the cross-section. On the other hand, if the theoretical problem is analyzed via the cohesive option, which omogenizes the composite material, two parameters $N_P^{(1)}$ and $N_P^{(2)}$ affect the kind of structural response. Physical similitude in the structural response is predicted when the dimensionless parameters are kept constant, althought the single mechanical and geometrical properties vary.

## NUMERICAL SIMULATIONS

The bridged crack model has been used to simulate some experimental results reported in [16]. Two different three point bending tests have been considered, related to beams having the same geometry and tension steel reinforcement. The two tests are denominated DR30 and DR32 in [16] and differ in the fiber volume ratio. While the beam DR30 is made by plain concrete, the beam DR32 has $1\%$ fiber volume ratio. The beams have rectangular cross section ($130 \times 203$ mm) and a total length of 2500 mm. The distance between the supports is 2250 mm (fig.2.a). The tension reinforcement is constituted by 2 $\varnothing$ 12 of high–strength steel bars. According to the model presented in this paper, the steel percentage is referred to the total cross section area, so that the steel percentage to be considered is $\rho = 0.86\%$.

The model produces as a result the values of the nondimensional bending moment and rotation as functions of the crack depth. For comparison with the experimental results these values have been converted into displacement versus load diagrams. The conversion is realized by considering the scheme of fig. 2.a, where a three point bending test is depicted. The displacement at midspan of the beam is supposed as given by the elastic part plus a rigid part due to the concentrated rotation of the cracked section. From the definition of nondimensional bending moment and rotation, we can write:

$$M_F = \tilde{M} K_{\mathrm{IC}} b h^{1.5}; \quad \phi = \frac{\tilde{\phi} K_{IC}}{E h^{0.5}}. \tag{10}$$

Consequently, the vertical load and displacement at midspan are given by:

$$P = \frac{4 M_F}{L}; \quad \delta = \delta_{el} + \delta_{\phi} = M_F \frac{L^2}{48 E^* I} + \frac{\phi L}{4}, \tag{11}$$

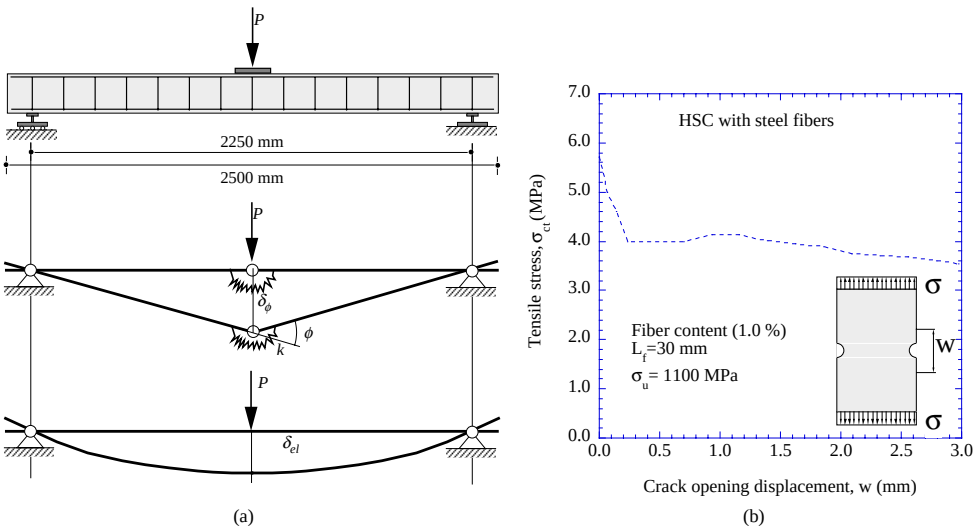


**Figure** 2. (a) Details of test beams and plastic hinge formation [16]; (b) response of high-strength concrete with fibers, after Noghabai [19].

where the inertia is related to the total cross section, $L$ is the span length, and $E^* = E/2.2$, $E$ being the conventional $28$ days static modulus. This assumption is known in the literature [4, 17] and takes into account the nonlinear material behavior in the zone ahead the crack tip. For the beam DR30 the modulus $E^*$ is then considered equal to 12.786 kN/mm$^2$.

The load vs. displacement diagram for the beam DR30 reported in [16] must be referred to a tension steel with a resistance higher than the reported one (617 N/mm$^2$). For this reason a tension steel reinforcement strength equal to 725 N/mm$^2$ has been considered in the simulations. We have assumed a matrix toughness $K_{IC}$=35.76 N/mm$^{3/2}$ and therefore $N_P^{(1)}$=2.484. The experimental and computed load vs. displacement diagrams are reported in fig. 3.a. The numerical simulation has been carried out using the bridging option, as the fibers were not present in this case. The results of the model do not catch the progressive decrease of the tangent modulus due to concrete damage, although reproduce closely the qualitative behavior of the structural member as well as the limit load. The latter result is due to assumed steel strength. The mechanical parameters adopted for the beam DR30, have been used for the simulation of the test DR32, where crimped steel fibers have been added to concrete. The steel fibers are characterized by a length equal to 50 mm, a diameter equal to 0.5 mm, a strength of 1050 N/mm$^2$ and are mixed with concrete with a percentage of $1\%$. The "effective density" of the fibers to be introduced in the model has been assumed equal to $0.2\%$, i.e. $1/5$ of the real one, for taking into account the random spatial distribution of the fibers inside the matrix and for the fact that the fibers are not bisected by the crack, but intersected at a random point along their length [18]. These assumptions provide a brittleness number $N_P^{(2)}$=0.84. Finally, a rigid-perfectly plastic law is considered for the fibers. This assumption finds justification considering

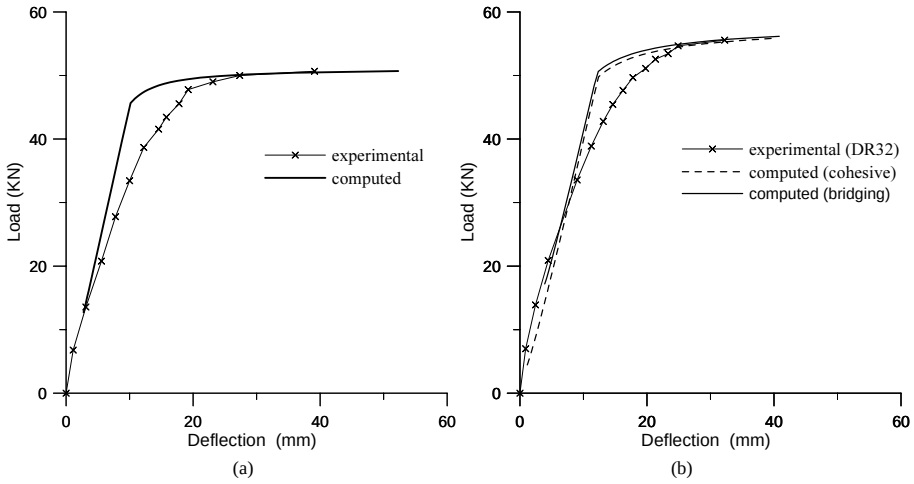


**Figure** 3. (a) Experimental and computed load vs. deflection diagrams for the beam DR30; (b) Experimental and computed load vs. deflection diagrams for the beam DR32 [16].

experimental results on similar steel fibers [19], fig. 3.b. As the experimental load vs. displacement diagrams have always positive slope with no slope discontinuities, the tension steel does not enter softening behavior and the fibers does not break along the crack depth, i.e., the crack opening is always less than the critical value $w_c$ and the cohesive zone extends along the whole crack depth. In fact, when the critical opening $w_c$ is achieved, the load vs. displacement diagram exhibits a softening branch, or at least a slope discontinuity. This is compatible with the fibers used in the experiment, as the crack opening at the maximum load is about $5\ \mathrm{mm}$. Consequently, the data used for the numerical simulation of the beam DR32 are the two brittleness numbers $N_P$, as the parameter $\tilde{w}_c$ is not influent, being $\tilde{w} < \tilde{w}_c$. Fig. 3.b reports the experimental load vs. displacement graphs compared to the computed ones, in both the cohesive or bridging option. The two curves are almost coincident, although in the two cases the nondimensional diagram bending moment versus crack depth markedly differs, fig. 4.a. For a given nondimensional moment, the crack depth is higher in the cohesive option. With reference to fig. 4.a, once the value $\tilde{M} = 1$ is fixed, a crack depth $\xi = 0.4376$ (bridging option) or $\xi = 0.5446$ (cohesive option) is found. The crack opening profiles are reported in fig. 4.b.

## CONCLUSIONS

The concurrent presence in a cementitious matrix of longitudinal bars and uniformly distributed fibers has been considered. Two different models have been proposed to simulate the flexural responce of a concrete element: the *bridged crack model* and the *cohesive crack model*. In the bridged crack model the composite material is theoretically simulated as a triphase material. Three distinct factors contribute to its global toughness: the cementitious matrix toughness $K_{IC}$, the fiber toughening mechanism, represented by the shielding effect $-K_{I\sigma}$ of the bridging tractions on the crack tip stress

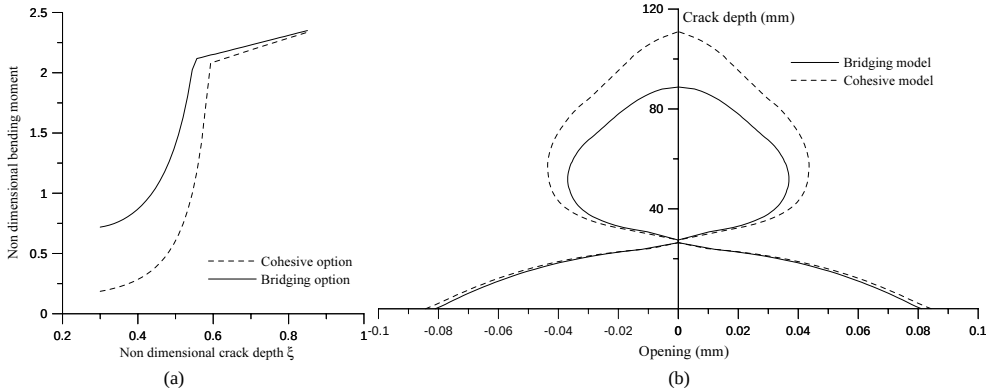


**Figure** 4. (a) Nondimensional bending moment vs. crack depth diagrams for the beam DR32; (b) Crack opening profile for the nondimensional bending moment $\tilde{M} = 1$.

intensification and the reinforcement bars toughening mechanism represented by the factor $-K_{Ii}$. In the cohesive-crack model, on the other hand, the composite material is theoretically simulated as a twophase material. The global toughening mechanism of the matrix and the fibers is defined: the toughening mechanism peculiar of the matrix and explicitly represented in the bridged crack model by $K_{IC}$ is merged with the toughening mechanisms developed in the process zone by the fibres.

Both the models reproduce satisfactorily the flexural behaviour of high-performance and/or fiber reinforced concrete members in bending. In particular, these models could represent a very useful tool for the study of mechanical properties and crack propagation regimes, based on concrete composition, typology and density of the fibers, distribution and characteristics of the longitudinal bars.

## ACKNOWLEDGEMENTS

The present research was carried out with the financial support of the Ministry of University and Scientific Research (MIUR), the National Research Council (CNR) and the EC-TMR Contract N$^o$ ERBFMRXCT960062.

## REFERENCES

1. Barenblatt, G.I. (1962) In Advances in Applied Mechanics, pp.55-129, Dryden, H.L., von Karman, T. (Eds.), Academic Press, New York.
2. Willis, J.R. (1967) *J. Mech. Phys. Solids* **15**, 151.
3. Rice, J.R. (1968) *Journal of Applied Mechanics* **35**, 379.
4. Carpinteri, A. (1981) *Materials and Structures* **14**, 151.
5. Carpinteri, A. (1984) *J. Struct. Engng. (ASCE)* **110**, 544.
6. Bosco, C., Carpinteri, A. (1992) *J. Engng. Mech. (ASCE)* **118**, 1564.
7. Bosco, C., Carpinteri, (1995) *J. Mech. Phys. Solids* **43**, 261.
8. Carpinteri, A., Massabó, R. (1996) *Int. J. Fract.* **81**, 125.
9. Carpinteri, A., Massabó, R. (1997) *Int. J. Solids Struct.* **34**, 2321.
10. Carpinteri, A., Massabó, R. (1997) *J. Engng. Mech. (ASCE)* **123**, 107.
11. Carpinteri, A., Ferro, G., Ventura, G., (2002) *Eng. Fract. Mech.*, in print.
12. Ferro, G. (2002) *Theor. Appl. Fract. Mech*, in print.
13. Okamura, H., Watanabe, K., Takano, T. (1975) *Eng. Fract. Mech.* **7**, 531.
14. Tada, H., Paris, P.C. and Irwin, G. (1973) *The Stress Analysis of Cracks Handbook*. Del Research Corp., St. Louis.
15. Buckingham, E. (1915) *Transactions ASME* **37**, 263.
16. Swamy, R.N., Al-Ta'an, S.A. (1981) *ACI Journal* **5**, 395.
17. Jenq, Y.S., Shah, S.P. (1986) *J. Engng. Mech. (ASCE)* **112**, 19.
18. Li, V.C., Wang, Y. and Backer, S. (1991) *J. Mech. Phys. Solids* **39**, 607.
19. Noghabai, K. (2000) *J. Struct. Engng. (ASCE)* **126**, 243.